



Shortlived absorption centers in plastic scintillators and their influence on the fluorescence light yield

W. Busjan¹, K. Wick^{*}, T. Zoufal

Institut für Experimentalphysik der Universität Hamburg, Bereich Teilchenphysik, Luruper Chaussee 149, D-22761 Hamburg, Germany

Received 26 March 1998; received in revised form 3 December 1998

Abstract

The process of radiation damage and its recovery were investigated during and after irradiation with X-rays. The absorption induced by X-rays in the scintillating fiber BCF-12 was measured in gas atmospheres with and without oxygen as a function of time, dose, dose rate and wavelength. The studies during irradiation showed several surprising effects: strong dose rate effects were observed. Shortlived absorption centers are formed during irradiation which decay within hours via a bimolecular reaction. The reaction constant for the decay decreases suddenly by a factor 200 in the moment when the concentration of oxygen dissolved in the fiber becomes zero. A kinetic model assuming three classes of absorption centers describes the dependence of the radiation induced absorption on dose and dose rate correctly. The influence of the shortlived absorption centers on the emitted fluorescence light yield was derived from the data as a function of dose rate. © 1999 Published by Elsevier Science B.V. All rights reserved.

PACS: 29.40.M; 42.81.Cn; 61.82.Pv; 78.20.C

Keywords: Scintillating fibers; Radiation damage; Dose rate effects; Optical absorption centers

1. Introduction

Radicals are created when plastic scintillators are used in a high dose rate environment. This effect diminishes the detector performance since radicals absorb fluorescence light. Although radicals are often macromolecules they are able to migrate through the polymer matrix. If no oxygen is available, migration is associated with rotational

motion of the polymer or is essentially a sequence of successive hydrogen abstraction reactions.



Here RH and R· denote polymer molecules and radicals, respectively. Radicals annihilate when two radicals come into close contact and interact.

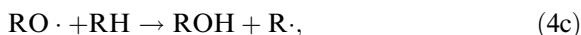
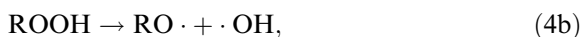
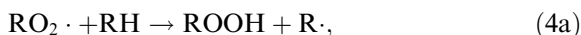


This bimolecular termination reaction is often called a second order process, it can proceed by cross-linking, disproportionation or recombination.

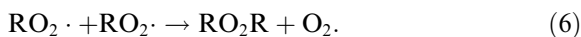
^{*} Corresponding author. Tel.: +49 40 899 82165; fax: +49 40 899 82101; e-mail: wick@maren.desy.de

¹ Present address. DESY, Hamburg.

Additional reaction channels are open when oxygen is available. The following simplified oxidation mechanism is similar to that proposed by Bolland [1]. A more detailed description of possible reactions between oxygen and radiation-induced radicals has been given by Clough et al. [2]. Radicals react rapidly with O_2 molecules forming peroxy radicals $RO_2\cdot$ as an intermediate state. Migration can now also occur via the following sequence of reactions:



The chain of reactions is terminated by one of the reactions (2), (5) or (6):



Reaction (3) is much faster than the others. Hence, one generally assumes that no radicals $R\cdot$ survive when oxygen is available. This is the basis of annealing of radiation damage in air.

At room temperature the radicals formed in polystyrene, the matrix of many plastic scintillators, are stable over periods of several weeks [3] if no oxygen is available. On the other hand short-lived absorption centers which decay within several hours were observed [4–7] during the irradiation of the scintillating fiber BCF-12 (BICRON) which also has a polystyrene matrix. These absorption centers are visible if one measures radiation damage during irradiation. Due to the short decay time it is difficult to detect them after the end of irradiation. A new broad absorption band peaked at the wavelength $\lambda = 580$ nm was observed, i.e., in a region where the additional absorption induced by radiation in pure polystyrene is very low. The investigation of the question whether these shortlived absorption centers may

affect the fluorescence light yield and the detector performance is one aim of the present work. This question is of interest for detector components using the BCF-12 fiber, for instance the SPACAL calorimeter in the H1 detector at HERA (DESY). For this purpose the overlap between the emission spectrum of the scintillator BCF-12 and the absorption spectrum of the shortlived absorption centers in the following denoted as R_2 , had to be determined. This means that the absorption spectra of R_2 and other absorption centers had to be separated.

Presently it is not known whether R_2 is a radical or not, but it behaves similar to most other radicals in polymers: R_2 decays via a second order process according to reaction (2), and secondly the decay of R_2 is much faster in the presence of oxygen than without oxygen [7]. Formation and subsequent annihilation ($R_2 + R_2 \rightarrow Y$) can be described by a simple differential equation

$$\frac{d[R_2]}{dt} = g_2 \cdot \varrho \cdot \dot{D} - k_2 \cdot [R_2]^2. \quad (7a)$$

The production rate is proportional to the dose rate \dot{D} and the decay rate is proportional to the square of the concentration $[R_2]$. t is the time, ϱ is the density of the scintillator and k_2 is the reaction constant for the decay of R_2 . g_2 is the chemical yield for the formation of R_2 , i.e., the number of produced absorption centers R_2 per absorbed energy ΔE (usually one uses $\Delta E = 100$ eV, in Eq. (7a) it is better to set $\Delta E = 1$ J). After a certain exposure time, an equilibrium state is achieved where production and decay rate of R_2 are equal ($d[R_2]/dt = 0$). The corresponding saturation concentration is given by

$$[R_2]_S = (g_2 \cdot \varrho \cdot \dot{D}/k_2)^{1/2} \propto \sqrt{\dot{D}}. \quad (7b)$$

Let us assume that $\sigma_2(\lambda)$ is the cross section² for the interaction of photons with wavelength λ and absorption centers R_2 . The additional absorption $\Delta\mu_2(\lambda)$ induced by the absorption centers R_2 can now be written as

² In most publications the extinction coefficient $\varepsilon(\lambda)$ is used instead of σ_2 . Both quantities are proportional to each other, $\varepsilon(\lambda) = N_A \cdot \sigma_2(\lambda)$, where N_A is AVOGADROS number.

$$\Delta\mu_2(\lambda) = [\mathbf{R}_2] \cdot \sigma_2(\lambda), \quad (8a)$$

$$\Delta\mu_2(\lambda) \approx \Delta\mu(\lambda) = \mu_{\text{irr}}(\lambda) - \mu_{\text{unirr}}(\lambda), \quad (8b)$$

where μ_{irr} and μ_{unirr} are the absorption coefficients of irradiated and unirradiated samples. Saturation of \mathbf{R}_2 ($\Delta\mu_2 \rightarrow \Delta\mu_{2S}$) is achieved at low doses ($D \simeq 20$ Gy) in BCF-12 [6], hence contributions from other absorption centers can be neglected in first approximation. The change of transmission of the fiber before (T_0) and during irradiation (T) can be expressed as

$$\begin{aligned} \frac{T(\lambda, \dot{D}) - T_0(\lambda)}{T_0(\lambda)} &\approx \exp \left[-\Delta\mu_{2S}(\lambda, \dot{D}) \cdot \ell \right] - 1 \\ &\approx -\Delta\mu_{2S}(\lambda, \dot{D}) \cdot \ell \propto \sqrt{\dot{D}} \end{aligned} \quad (9)$$

if $\Delta\mu_{2S} \cdot \ell \ll 1$. ℓ is the path length of the light in the (homogeneously) irradiated part of the fiber.

Let us briefly summarize the effect of shortlived absorption centers \mathbf{R}_2 on the calibration of a detector in a high dose rate environment. The transmission of the fiber decreases within the first hours of the irradiation until saturation of \mathbf{R}_2 is achieved ($\Delta\mu_2 \rightarrow \Delta\mu_{2S}$). As a consequence the detector calibration will change slightly depending on the dose rate produced by the beam correlated background in the detector. A quantitative prediction of this effect is given in Section 4.4. This is of interest since modern detectors used in high energy physics mostly need a calibration accuracy of about $\pm 1\%$.

2. Experimental procedure

Systematic studies were performed for the BCF-12 fiber which emits blue fluorescence light. In an additional experiment the scintillating fiber SCSF81(Y7) (KURARAY) emitting green light was investigated. Both fibers have a polystyrene core and a PMMA (polymethyl methacrylate) cladding.

The BCF-12 fibers were mounted in a vacuum chamber with quartz windows which could be filled with different gas atmospheres. The diameter of the fiber was 1 mm, the length of its irradiated part was 6.5 cm. A 100 kV X-ray tube was used to perform the irradiations, while the dose rate was

varied in the range 7–42 Gy/h by means of a rotating lead shutter. The temperature inside the vacuum chamber was stabilized using a water cooling system. The stability requirements during the experiment were very high, since the maximum duration of the measurements was about 11 days.

The light transmission in the fiber was measured before, during and after irradiation. From these data the radiation induced absorption $\Delta\mu(\lambda, t)$ (see Section 1) was derived as a function of time t and wavelength λ . The fibers were covered with black colour in order to suppress transmission of light in PMMA cladding. Details of the experimental setup and the method were described elsewhere [4,5,7].

Due to the continuous energy spectrum of X-rays and several absorbers between source and fiber it was difficult to determine the dose absorbed during irradiation. Doses absorbed in the scintillator and different types of dosimeters were calculated using the code PHOTCOEF [8]. Since the absolute intensity of the X-ray source was not well known, additional measurements were performed with the dosimeter Amber Perspex 3042D (HARWELL/BICRON) which allowed to determine absolute doses more accurately. The systematic error of the absolute doses is about $\pm 7\%$, the relative uncertainty of different doses is much less ($\pm(1-2)\%$). The errors given in the following include only the relative uncertainty of the doses, not the systematic error.

3. Kinetic model for BCF-12

In this section a kinetic model is discussed which describes the measured radiation induced absorption $\Delta\mu$ as a function of the relevant parameters (time t , dose D , dose rate \dot{D} and wavelength λ). Only the kinetics will be considered, the nature of the different absorption centers will be discussed in Section 5.1. Most earlier studies analyzed only the behaviour after irradiation, however, a realistic model has to describe the whole process during and after irradiation. Many investigations have shown that the availability of oxygen accelerates the annealing process considerably. This means that the concentration $[\text{O}_2]$ of oxygen

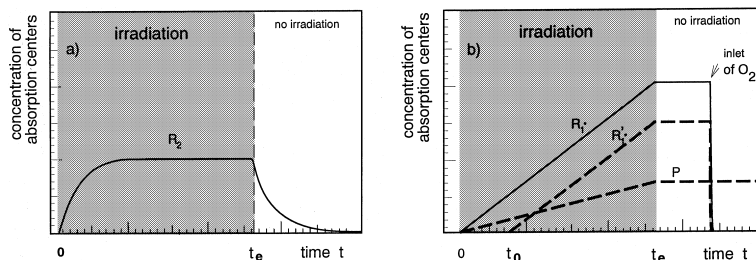


Fig. 1. Formation and decay of different types of absorption centers during and after irradiation in argon atmosphere (schematic representation). (a) R_2 are unstable absorption centers which decay via a second order process ($R_2 + R_2 \rightarrow X$). (b) P are stable absorption centers, while the radicals $R_1 \cdot$ are stable only in the absence of oxygen. The dotted line ($R_1' \cdot$) is plotted under the assumption that the oxygen dissolved in the fiber is consumed after a time t_0 .

dissolved in the scintillator is an essential parameter.

The basic assumptions of the kinetic model are the following.

(1) Three classes of absorption centers contribute to the measured radiation induced absorption. Each one has its characteristic absorption spectrum. In the present experiment absorption centers can be distinguished if they develop differently as a function of time and behave differently in gas atmospheres with and without oxygen. The absorption centers are denoted as P , $R_1 \cdot$ and R_2 when no oxygen is dissolved in the scintillator ($[O_2] = 0$) and P' , $R_1' \cdot$ and R_2' in the case $[O_2] \neq 0$. (In the following quantities with prime refer to the case $[O_2] \neq 0$ while those without prime refer to the case $[O_2] = 0$.) The stable absorption centers (P , P') are responsible for the permanent transmission damage while the annealable damage is caused by radicals ($R_1 \cdot$, $R_1' \cdot$) and by the shortlived absorption centers (R_2 , R_2') mentioned in Section 1. The measured radiation induced absorption $\Delta\mu$ can then be written as a sum $\Delta\mu = \Delta\mu_1 + \Delta\mu_2 + \Delta\mu_p$ (or correspondingly $\Delta\mu' = \Delta\mu'_1 + \Delta\mu'_2 + \Delta\mu'_p$). In the following text the slope parameters

$$\Sigma_i(\lambda) = \frac{d[\Delta\mu_i(\lambda, D \approx 0)]}{dD} \quad \text{for } i = 1, 2, P \quad (10)$$

will be used. Each absorption center i has its characteristic absorption "spectrum" $\Sigma_i(\lambda)$. Σ_i is proportional to the chemical yield g_i of absorption center i (see Eq. (13)).

(2) The time dependence of the concentrations of the different absorption centers and their contributions $\Delta\mu_i$ ($i = 1, 2, P$) to the induced absorption are plotted schematically in Figs. 1 and 2. A brief discussion follows:

- Stable absorption centers (P , P') can be generated in the primary collision between particles and polymer molecules as well as during annealing according to Eqs. (2)–(6). In the present analysis only the first process is taken into account, i.e., we assume that the permanent damage rises linearly with dose during irradiation ($\Delta\mu_p = \Sigma_p \cdot D$) and remains constant after irradiation. This simple assumption may be sufficient since the contribution of stable absorption centers (P , P') is very small in the

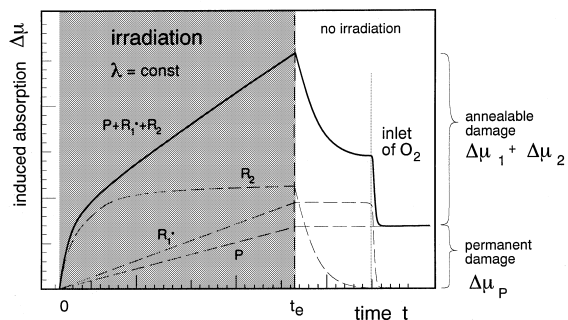


Fig. 2. The additional absorption $\Delta\mu$ induced in the scintillator BCF-12 during irradiation in argon atmosphere. The stable absorption centers P are responsible for the permanent damage $\Delta\mu_p$, while the annealable damage ($\Delta\mu_1 + \Delta\mu_2$) is caused by $R_1 \cdot$ and R_2 . Rapid annealing occurs after inlet of oxygen.

present experiment. A linear dependence of the permanent damage on the dose D was observed for polysterene [9] and the plastic scintillator SCSN-38 [10].

- Radicals $R\cdot$ (here denoted as $R_1\cdot$) can be considered as stable molecular fragments under the conditions of the present experiment (ambient temperature, relatively low doses $D \leq 2.5$ kGy, annealing time ≤ 10 days) if no oxygen is available ($\Delta\mu_1 = \Sigma_1 \cdot D$). Radicals strongly absorb blue and UV light. If oxygen is dissolved in the scintillator the same type of radicals will be formed ($R_1\cdot = R'_1\cdot$), however they will decay rapidly according to reactions (3)–(6). Hence, one expects that the radical concentration $[R'_1\cdot]$ vanishes and that $\Delta\mu'_1 = \Sigma'_1 \cdot D = 0$ if $[O_2] \neq 0$. In the case $[O_2] = 0$ the contributions of the absorption centers P and $R_1\cdot$ cannot be distinguished during irradiation, after irradiation they can be separated if one introduces oxygen into the vacuum chamber (see Fig. 1(b)). This has no influence on the stable absorption centers P, but the radicals $R_1\cdot$ will decay rapidly.
- Shortlived absorption centers (R_2, R'_2) were observed in both cases with and without dissolved oxygen. However, the decay times in both cases were completely different. Hence, it is one aim of the present experiment to see whether the two species R_2 and R'_2 are identical or not.

Let us now consider more accurately the shortlived absorption centers R_2 decaying via a second order process (2). The solution of Eq. (7a) is well known. Using Eq. (8a) it can be written during irradiation ($0 \leq t \leq t_e$):

$$\Delta\mu_2(\lambda, \dot{D}, t) = \Delta\mu_{2S}(\lambda, \dot{D}) \cdot \tanh(t \cdot \sqrt{\dot{D} \cdot \kappa_2}). \quad (11a)$$

For the saturation value $\Delta\mu_{2S}$ one can write

$$\Delta\mu_{2S}(\lambda, \dot{D}) / \sqrt{\dot{D}} = \Sigma_2(\lambda) / \sqrt{\kappa_2}. \quad (11b)$$

The unknown parameters (κ_2, Σ_2) are related to the parameters $(k_2, g_2, \sigma_2(\lambda))$ defined in Section 1:

$$\kappa_2 = g_2 \cdot \varrho \cdot k_2, \quad (12)$$

$$\Sigma_2(\lambda) = g_2 \cdot \varrho \cdot \sigma_2(\lambda). \quad (13)$$

At very low doses ($D = \dot{D}t \ll (\dot{D}/\kappa_2)^{1/2}$) one obtains from Eqs. (11a) and (11b)

$$\Delta\mu_2(\lambda, D) \approx \Sigma_2(\lambda) \cdot D. \quad (11c)$$

The corresponding solution after irradiation ($t > t_e$) is

$$\Delta\mu_2(\lambda, \dot{D}, D, t) = \left[\Delta\mu_2(\lambda, \dot{D}, t_e)^{-1} + \beta_2(\lambda) \cdot (t - t_e) \right]^{-1}, \quad (14)$$

where

$$\beta_2(\lambda) = k_2 / \sigma_2(\lambda) = \kappa_2 / \Sigma_2(\lambda). \quad (15)$$

An important result obtained for the bimolecular reaction (2) is that the time dependence of $\Delta\mu_2$ during and after irradiation can be described according to Eqs. (11a)–(11c), (14) and (15) with only two free parameters (κ_2, Σ_2) .

The above Eqs. (11a)–(15) are written for the case $[O_2] = 0$. If oxygen is dissolved in the sample ($[O_2] \neq 0$) similar equations hold as has been shown in Ref. [6]. Since the parameters are not the same one has to replace the quantities $(\kappa_2, \Sigma_2, \beta_2, \Delta\mu_2)$ by other ones $(\kappa'_2, \Sigma'_2, \beta'_2, \Delta\mu'_2)$. The time dependence during and after irradiation is plotted schematically in Fig. 1(a): the concentration of absorption centers $[R_2]$ and the radiation induced absorption $\Delta\mu_2 = [R_2] \cdot \sigma_2(\lambda)$ saturate after a short exposure time.

The radiation induced absorption $\Delta\mu$ in the case $[O_2] = 0$ can now be written as a sum of three terms which are due to the three absorption centers P, $R_1\cdot$ and R_2 as is plotted schematically in Fig. 2:

$$\Delta\mu(\lambda, \dot{D}, D, t) = \left[\Sigma_P(\lambda, \dot{D}) + \Sigma_1(\lambda, \dot{D}) \right] \cdot D + \Delta\mu_2(\lambda, \dot{D}, D, t). \quad (16a)$$

Eq. (16a) holds during ($D = \dot{D} \cdot t$) and after irradiation ($\dot{D} = 0$), this is the reason why $\Delta\mu$ is written as a function of four parameters. $\Delta\mu_2$ is given by Eqs. (11a), (11b) and (14), respectively. If oxygen is dissolved in the fiber ($[O_2] \neq 0$) for instance when the fiber is irradiated in air, Eq. (16a) has to be replaced by a similar equation with other parameters

$$\Delta\mu'(\lambda, \dot{D}, D, t) = \left[\Sigma'_P(\lambda, \dot{D}) + \Sigma'_1(\lambda, D) \right] \cdot D + \Delta\mu'_2(\lambda, \dot{D}, D, t). \quad (17)$$

In some experiments oxygen was dissolved in the fiber although the irradiations were performed in argon. This occurs if the fiber was stored in air before irradiation. After exposure to a certain dose $D_0 = \dot{D} \cdot t_0$, the dissolved oxygen will be completely consumed due to reactions of the type (3)–(6). In this case (see Fig. 1(b)) the radical concentration $[R_1 \cdot]$ will be zero for doses $D \leq D_0$ ($t \leq t_0$). During irradiation and for doses $D \geq D_0$ Eq. (16a) has to be replaced by

$$\begin{aligned} \Delta\mu(\lambda, \dot{D}, D, t) = & \Sigma_P(\lambda, \dot{D}) \cdot D \\ & + \Sigma_1(\lambda, \dot{D}) \cdot (D - D_0) \\ & + \Delta\mu_{2S}(\lambda, \dot{D}) \cdot \tanh \left[\sqrt{\kappa_2 / \dot{D}} \cdot (D - D_0) \right]. \end{aligned} \quad (16b)$$

The curve $\Delta\mu(t)$ shows a characteristic kink [7] at dose D_0 from which D_0 can be determined. For a fixed wavelength λ Eqs. (16b) and (17) contain 4 parameters ($\Sigma_1, \Sigma_2, \Sigma_P, \kappa_2$) for the case $[O_2] = 0$ and 5 parameters ($\Sigma'_1, \Sigma'_2, \Sigma'_P, \kappa'_2, D_0$) for the case $[O_2] \neq 0$ which have to be determined from experiment.

From the ESR (electron spin resonance) studies it is well known that peroxy radicals $RO_2 \cdot$ are produced in irradiated polymers if oxygen is available ($[O_2] \neq 0$). It has been assumed in Eq. (17) that these radicals do not absorb visible light. This assumption will be tested experimentally.

4. Experimental results

The kinetics of BCF-12, i.e., the time dependence of the radiation induced absorption $\Delta\mu$ for selected wavelengths is discussed separately for irradiations in argon (Section 4.1) and air (Section 4.2). The absorption spectra of the different types of absorption centers detected in BCF-12 is studied in Section 4.3. An important item is the emitted fluorescence light yield and its dependence on the radiation induced absorption, this point will be discussed in Section 4.4.

4.1. Irradiations in argon

From the transmission measurement the radiation induced absorption $\Delta\mu(\lambda, t)$ is derived as a

function of the wavelength λ and the time t during and after irradiation. A representative example is plotted in Fig. 3. The absorption spectrum (Figs. 3(b) and (c)) is characterized by two broad absorption bands peaked at wavelengths $\lambda = 580$ nm

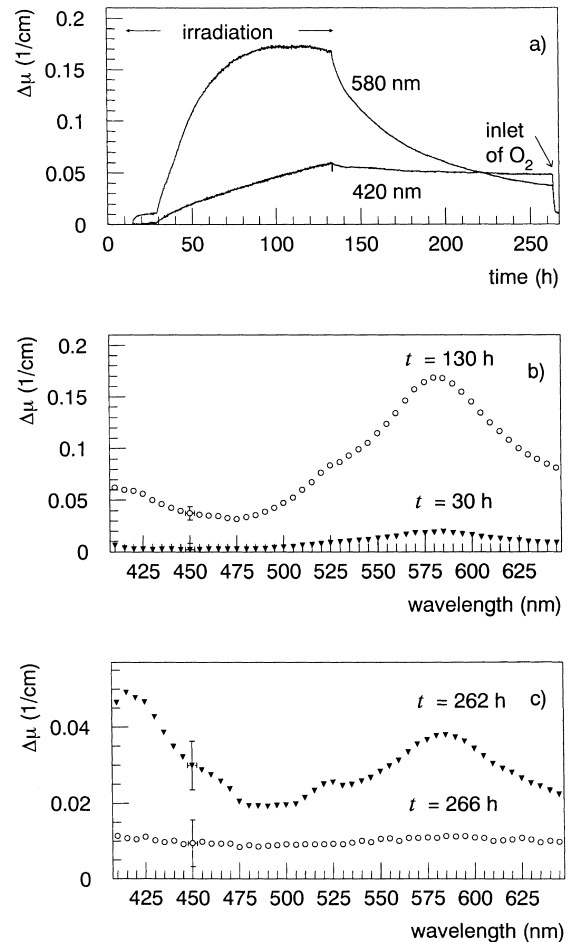


Fig. 3. Typical experimental result obtained during and after irradiation of the scintillating fiber BCF-12 in argon atmosphere ($D = 1.26$ kGy, $\dot{D} = 10.5$ Gy/h, duration of experiment ~ 11 days). The radiation induced absorption $\Delta\mu$ is plotted as a function of time (a) and wavelengths (b) and (c). (a) The time dependence is completely different for the two representative wavelengths $\lambda = 420$ and 580 nm. The arrows indicate the exposure time (120 h) (b) and (c) present the absorption spectra measured at different times t during (b) and after irradiation (c). The spectra are plotted at selected times (see (a): $t = 30$ h (kink), $t = 130$ h (end of irradiation), $t = 262$ h (moment before inlet of oxygen), $t = 266$ h (after 4 h of annealing)). The error bars at 450 nm in (b) and (c) represent the systematic error.

and $\lambda \lesssim 420$ nm, respectively. The time dependence for the two bands is completely different (Fig. 3(a)) indicating that the two bands are due to different kinds of absorption centers. A comparison with Figs. 1 and 2 shows that shortlived absorption centers (R_2) dominate at 580 nm while the behaviour at 420 nm is typical for stable absorption centers at least when no oxygen is present.

The origin of the kinks observed at time $t = 30$ h in both curves of Fig. 3(a) has been described in Section 3 and in Ref. [7]. The BCF-12 fiber was stored in air before irradiation. The oxygen dissolved in the fiber at the beginning of irradiation is consumed due to reactions with radicals, and the kink is observed just at the moment when the oxygen concentration $[O_2] = 0$ is reached. In the experiment this occurs after an absorbed dose $D_0 = 150$ Gy. This clearly demonstrates the advantage of oxygen: rapid annealing of radiation damage during irradiation occurs only when oxygen is dissolved in the sample. After consumption of oxygen the induced absorption increases much more strongly than before. This is due to the fact that the radicals $R_1\cdot$ can only exist when $[O_2] = 0$. It explains also the second sharp kink at $t = 262$ h when oxygen was introduced into the vacuum chamber. The radicals $R_1\cdot$ and the absorption centers R_2 decay rapidly when oxygen diffuses into the fiber, only the permanent damage remains – this first example demonstrates that the measurement of absorption during irradiation allows to register valuable details of the process which often cannot be detected after irradiation.

In the following part of this section the time dependence of absorption will be considered for $\lambda_0 = 580$ nm, i.e., for the wavelength where the induced absorption has a maximum. Here are the best conditions to understand the kinetics of the shortlived absorption centers R_2 . Fig. 4(a) presents the results obtained during irradiations in argon at different dose rates. There are two reasons why the shape of the two measured curves are so different: there is a strong dose rate effect and secondly the parameter D_0 is different for the two curves. From the kink in the lower curve ($\dot{D} = 10.5$ Gy/h) one obtains $D_0 = 150$ Gy while for the upper curve ($\dot{D} = 42$ Gy) $D_0 = 0$ holds. As mentioned above, D_0 is the dose which is necessary to consume the

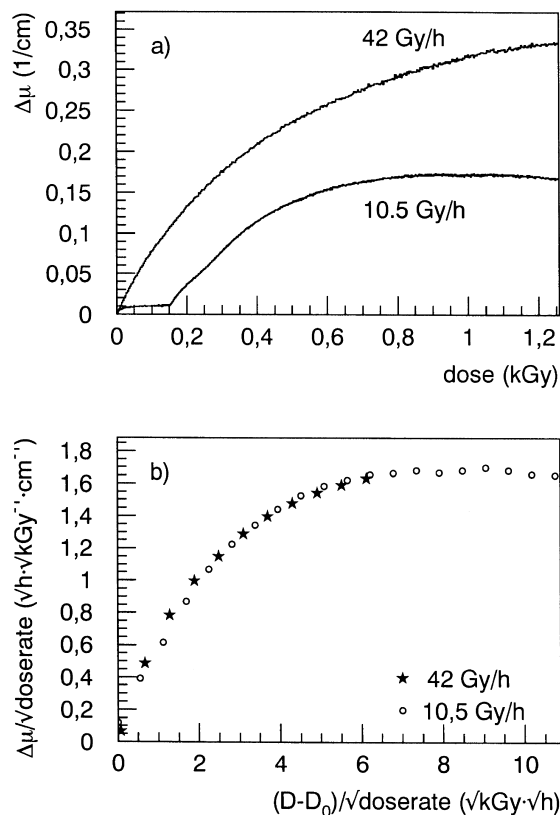


Fig. 4. (a) The absorption $\Delta\mu(\lambda = 580$ nm) induced during irradiation of the BCF-12 fiber in argon is strongly dose rate dependent ($\dot{D} = 10.5$ and 42 Gy/h, respectively, dose $D = 1.26$ kGy). (b) The results of the two experiments plotted in (a) agree completely if the data is plotted in the scale invariant form (Eq. (18)).

oxygen dissolved in the fiber, and this quantity depends of course on the prehistory of the fiber before irradiation [7].

It is interesting that Eq. (11a) describing the induced absorption predicted by the second order process during irradiation can be written in a scale invariant form

$$\frac{\Delta\mu_2(\lambda, \dot{D}, D = \dot{D}t)}{\sqrt{\dot{D}}} = \frac{\Delta\mu_{2S}}{\sqrt{\dot{D}}} \cdot \tanh\left(\sqrt{\kappa_2} \cdot \frac{(D - D_0)}{\sqrt{\dot{D}}}\right). \quad (18)$$

According to Eq. (11b) $\Delta\mu_{2S}/\sqrt{\dot{D}}$ should only depend on the wavelength λ . In order to test Eq. (18)

the measured quantities $\Delta\mu/\sqrt{D}$ are plotted in Fig. 4(b) as a function of $(D - D_0)/\sqrt{D}$. As one can see the two curves for dose rates $\dot{D} = 10.5$ and 42 Gy/h, respectively, agree completely. This is a very successful confirmation of the investigated model. There is another reason why this result is of interest: from the curve of Fig. 4(b) one can easily predict the radiation induced absorption $\Delta\mu(\lambda_0 = 580 \text{ nm})$ for arbitrary doses and dose rates.

Figs. 4(a) and (b) show that $\Delta\mu(\lambda_0 = 580 \text{ nm})$ converges at relatively low doses to a constant value. From a comparison of Figs. 2 and 4 one can conclude that the influence of the shortlived absorption centers (R_2) dominates and that the contributions from other absorption centers (R_1 , P) are negligible at $\lambda_0 = 580 \text{ nm}$ ($\Sigma_1(\lambda_0) = \Sigma_P(\lambda_0) = 0$). This is the reason why in the analysis of Fig. 4 only the shortlived absorption centers (R_2) were taken into account, one can set $\Delta\mu(\lambda_0) = \Delta\mu_2(\lambda_0)$.

In the next step the time dependence of $\Delta\mu$ will be quantitatively compared with the model discussed in Section 3. Eqs. (11a)–(11c) and (14) de-

scribing production and annihilation of R_2 depend on two parameters ($\kappa_2, \Sigma_2(\lambda)$). However, it is difficult to determine these quantities by means of a least square fit, since they are strongly correlated as can be seen from Eqs. (11b), (14) and (15). From the experimental point of view it is better to use the quantities $(\Delta\mu_{2S}/\sqrt{D}, \kappa_2)$ for parameterization. $\Delta\mu_{2S}$ is the saturation value of the induced absorption. According to Eq. (11b) $\Delta\mu_{2S}/\sqrt{D}$ should only depend on the wavelength, not on dose and dose rate.

The results of three independent experiments performed under different experimental conditions (dose $D = 50 - 1260$ Gy, dose rate $\dot{D} = 8.4 - 42$ Gy/h) are presented in Fig. 5. In all cases the fibers were stored in argon atmosphere during and after irradiation. At the beginning of the irradiations the concentration of oxygen dissolved in the fiber was in one case $[O_2] = 0$ (Fig. 5(a)) and in two cases $[O_2] \neq 0$ (Figs. 5(b) and (c)). The concentration $[O_2]$ depends on the fact whether the fiber was stored in argon or in air before irradiation.

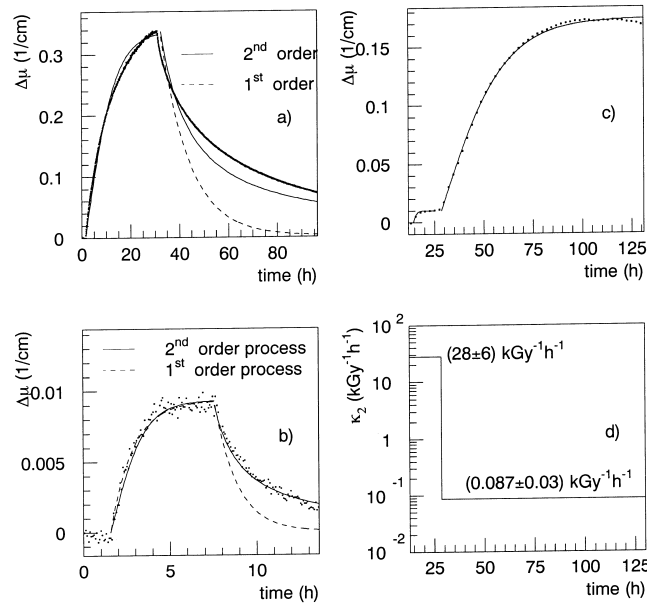


Fig. 5. (a)–(c) Time dependence of the induced absorption $\Delta\mu(\lambda = 580 \text{ nm})$ of BCF-12 measured in argon under different experimental conditions: (a) $D = 1260$ Gy, $\dot{D} = 42$ Gy/h, $[O_2] = 0$; (b) $D = 50$ Gy, $\dot{D} = 8.4$ Gy/h, $[O_2] \neq 0$; (c) $D = 1260$ Gy, $\dot{D} = 10.5$ Gy/h, $[O_2] \neq 0$ for $t < 30$ h, $[O_2] = 0$ for $t \geq 30$ h. The behaviour during and after irradiation can be well described by a second order but not by a first order process ((a) and (b)). (d) The reaction parameter κ_2 decreases suddenly by a factor of about 300 when the oxygen dissolved in the fiber is consumed by reactions with radicals ($[O_2] \rightarrow 0$ at $t = 30$ h in (c)).

First results of the analysis can be summarized as follows.

- Formation and annihilation of shortlived absorption centers R_2 can be fitted with only two free parameters if one supposes a second order decay process ($R_2 + R_2 \rightarrow X$) as can be seen from Figs. 5(a) and (b). A decay via a first order process ($R_2 \rightarrow Y$) can be excluded (Figs. 5(a) and (b)).
- The reaction parameter κ_2 decreases suddenly by a factor (200–300) when the oxygen concentration reaches the limit $[O_2] \rightarrow 0$ (Fig. 5(d)).

A confirmation of the latter statement can be obtained from Fig. 5(c). The kink at $t = 30$ h indicates that the oxygen dissolved in the fiber is consumed. Hence, the two regions with $[O_2] \neq 0$ ($t < 30$ h) and $[O_2] = 0$ ($t > 30$ h) were fitted independently using the same formula (11a). The result is plotted in Fig. 5(d): the reaction parameter κ_2 decreases at $t = 30$ h from $\kappa'_2 = 28 \text{ kGy}^{-1} \text{ h}^{-1} \rightarrow \kappa_2 = 0.087 \text{ kGy}^{-1} \text{ h}^{-1}$.

In order to test this result a further experiment presented in Fig. 5(b) was performed in argon. In this case the irradiation was stopped at a relatively low dose ($D = 50$ Gy) before the dissolved oxygen was consumed. As expected formation and decay of R_2 can be reproduced with the high value of the reaction parameter ($\kappa'_2 = 31 \pm 6 \text{ kGy}^{-1} \text{ h}^{-1}$). A similar result ($\kappa'_2 = 32 \text{ kGy}^{-1} \text{ h}^{-1}$, $\Delta\mu'_{2s}/\sqrt{\dot{D}} = 0.16 \text{ cm}^{-1} \text{ kGy}^{-1/2} \text{ h}^{1/2}$) was obtained for an irradiation in air [6].

The second parameter $\Delta\mu_{2s}/\sqrt{\dot{D}}$ at $\lambda_0 = 580$ nm depends also strongly on the fact whether oxygen is available or not as can be seen from Fig. 6, but in agreement with Eq. (11b) the ratio does not depend on the dose rate \dot{D} . The analysis of the data measured in argon according to Eqs. (16a), (16b) and (17) yields the parameters given in Table 1 and in addition $\Sigma_1(\lambda_0) = \Sigma_P(\lambda_0) = \Sigma'_1(\lambda_0) = \Sigma'_P(\lambda_0) = 0$. The parameter D_0 will be determined in Section 4.2. For the two parameters describing production (Σ_2) and decay (κ_2) of the shortlived absorption centers R_2 we obtain the following surprising result: the rate parameter κ_2 for the bimolecular reaction $R_2 + R_2 \rightarrow X$ decreases suddenly by a factor $\kappa'_2/\kappa_2 = 204 \pm 50$, when the limit $[O_2] \rightarrow 0$ is reached, while $\Sigma_2(\lambda_0)$ remains constant ($\Sigma_2(\lambda_0) \approx \Sigma'_2(\lambda_0)$). The parameter $\Delta\mu_{2s}(\lambda_0)/\sqrt{\dot{D}}$

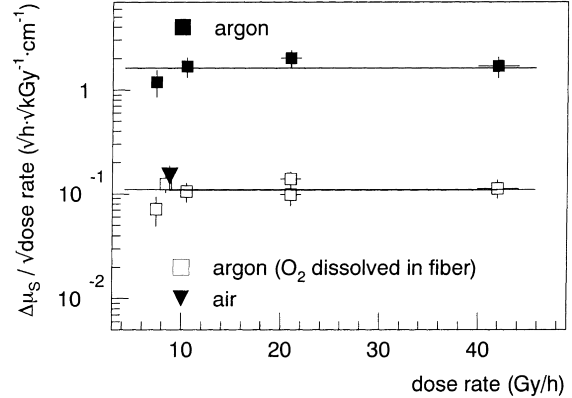


Fig. 6. The ratio $\Delta\mu_{2s}/(\dot{D})^{1/2}$ ($\Delta\mu_{2s}$ = saturation value of the absorption induced in BCF-12 at $\lambda = 580$ nm) is plotted as a function of the dose rate \dot{D} for different irradiations in argon (with and without dissolved oxygen) and in air.

decreases by a factor 13. This is in agreement with Eq. (11b) from which one obtains a factor $(\kappa'_2/\kappa_2)^{1/2} = 14 \pm 2$. These results are confirmed in Section 4.3, where the data for other wavelengths will be analyzed.

4.2. Irradiations of BCF-12 in air

The behaviour of plastic scintillators during irradiations in air is more complicated than in argon since the diffusion of oxygen plays an important role. Earlier investigations [11] of plastic scintillators have shown that the observed absorption $\Delta\mu$ induced by the radiation may depend

Table 1
Parameters characterizing the time dependence of the induced absorption $\Delta\mu_2(\lambda_0, t)$ for the shortlived absorption centers R_2 at $\lambda_0 = 580$ nm.

| | $[O_2] = 0$ | $[O_2] \neq 0$ |
|---|-------------------|-----------------|
| κ_2 ($\text{kGy}^{-1} \text{ h}^{-1}$) | 0.152 ± 0.023 | 31 ± 6 |
| $\Delta\mu_{2s}(\lambda_0)/\sqrt{\dot{D}}$ ($\text{cm}^{-1} \text{ kGy}^{-1/2} \text{ h}^{1/2}$) | 1.62 ± 0.19 | 0.11 ± 0.02 |
| $\Sigma_2^{\text{calc}}(\lambda_0)$ ($\text{cm}^{-1} \text{ kGy}^{-1}$) | 0.63 ± 0.10 | 0.61 ± 0.15 |
| $\Sigma_2^{\text{exp}}(\lambda_0)$ ($\text{cm}^{-1} \text{ kGy}^{-1}$) | 0.70 ± 0.12 | 0.72 ± 0.15 |

on the dose rate \dot{D} . An important parameter is the so-called critical dose rate \dot{D}_{crit} which depends on the oxygen pressure, the basic material, the thickness of the scintillator and on the fiber cladding. At low dose rates ($\dot{D} < \dot{D}_{\text{crit}}$) the O_2 molecules diffusing into a scintillating fiber can reach its center, and oxygen will be available ($[\text{O}_2] \neq 0$) in the whole fiber. In this case radicals $\text{R}_1\cdot$ will decay at once, annealing will occur during irradiation. In good approximation the decay of absorption centers ($\text{R}_1\cdot$, R_2) depends only on the fact whether oxygen is available or not and only weakly on the absolute concentration $[\text{O}_2]$ of dissolved oxygen. Hence, the results obtained during an irradiation in air and an irradiation in argon with $[\text{O}_2] \neq 0$ agree quite well in the case $\dot{D} < \dot{D}_{\text{crit}}$ as was mentioned in Section 4.1. At high dose rates ($\dot{D} > \dot{D}_{\text{crit}}$) all O_2 molecules diffusing from outside into the fiber will be bound by radicals before they reach its center. The consequence is a non-uniform distribution of absorption centers. In the center of the fiber there is an oxygen free zone with high concentrations $[\text{R}_1\cdot]$, $[\text{R}_2]$, while the concentration of absorption centers will be much lower in the surface region where $[\text{O}_2] \neq 0$.

In Fig. 7(a) the induced absorption $\Delta\mu(\lambda = 580 \text{ nm})$ is plotted for two independent irradiations at similar dose rates, one was performed in air, the other one in argon. The second curve is part of the curve presented in Fig. 3(a). In both cases the fiber was stored in air under normal conditions (room temperature, $p \approx 1 \text{ bar}$) before the experiment started. Hence, in both cases oxygen is dissolved in the fibers and the curves in Fig. 7(a) are very similar until the oxygen is consumed at least in the center of the fiber. This is the moment when the kinks in both curves (indicated by the hatched lines) occur. An attempt is made in Fig. 7(b) to explain the processes in the fiber and the time dependence of $\Delta\mu$ qualitatively for the irradiation in air. We assume that the dose rate $\dot{D} = 8.8 \text{ Gy/h} > \dot{D}_{\text{crit}}$. At the end of phase 1 corresponding to an absorbed dose D_0 the dissolved oxygen is consumed in the center of the fiber. The diameter of the oxygen free zone increases in phase 2, until it reaches an equilibrium value (phase 3). Since there is no annealing in the oxygen free zone we expect an increase of induced absorption $\Delta\mu$ for

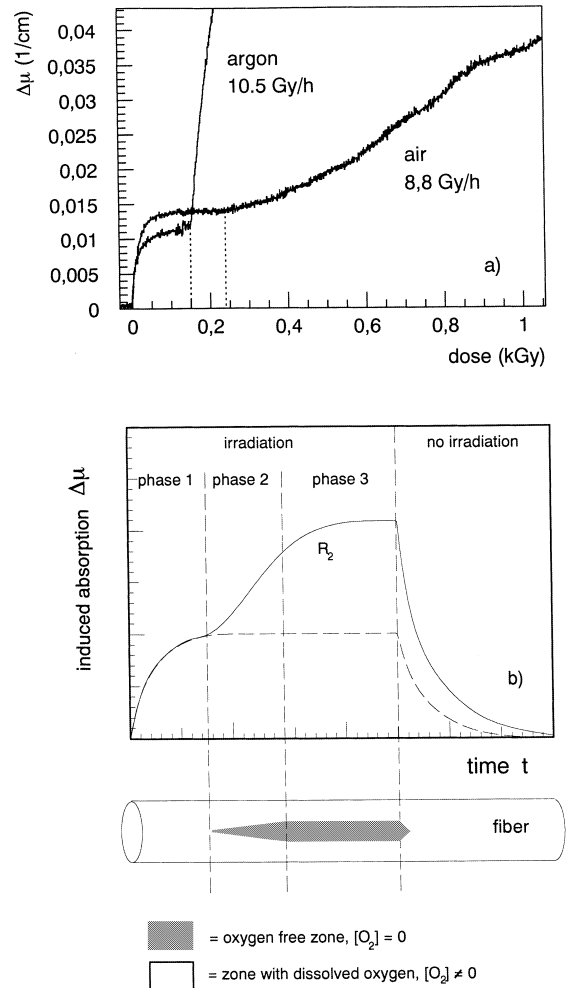


Fig. 7. (a) Comparison of the induced absorption $\Delta\mu(\lambda = 580 \text{ nm})$ for two irradiations performed in air ($\dot{D} = 8.8 \text{ Gy/h}$, $D = 1.1 \text{ kGy}$) and in argon ($\dot{D} = 10.5 \text{ Gy/h}$, $D = 1.26 \text{ kGy}$). The oxygen dissolved in the fiber at the beginning of the irradiation is consumed after exposure to doses of 150 and 240 Gy, respectively. The behaviour during irradiation in air is explained qualitatively in (b). (b) During irradiation in air the O_2 molecules which are bound chemically due to reactions with radicals can be replaced by O_2 diffusion into the fiber. As a consequence of the two competing processes one will obtain at high dose rates ($\dot{D} > \dot{D}_{\text{crit}}$) an oxygen free zone in the center of the fiber (lower part of (b)) and a non-uniform distribution of absorption centers ($\text{R}_1\cdot$, R_2).

$D > D_0$. During irradiation in argon no oxygen can diffuse from outside into the fiber. Consequently for $D > D_0$ the whole fiber will be oxygen free and the slope $d(\Delta\mu)/dD$ will be much

higher than during irradiation in air (see Fig. 7(a)).

From the kink one can determine the dose D_0 which is necessary to consume the O_2 molecules dissolved in the fiber. From the measurement in argon one obtains only a lower limit ($D_0 > 150$ Gy) since part of the O_2 molecules can diffuse out of the fiber within the first 30 h (see Fig. 3(a)) of the experiment. From independent measurements we obtain for BCF-12 stored in air before irradiation

$$D_0 = (350 \pm 100) \text{ Gy.}$$

From D_0 one can further estimate the chemical yield $g(-O_2)$ for BCF-12, i.e., the number of O_2 molecules consumed per unit of absorbed energy

$$g(-O_2) = \frac{C_s}{\varrho \cdot D_0},$$

where ϱ is the density of BCF-12 and C_s is the saturation concentration of O_2 molecules under normal conditions in air. If we assume that both quantities are the same as in pure polystyrene ($C_s = 8.8 \cdot 10^{17}/\text{cm}^3$ according to Ref. [17]) one obtains under the conditions of the present experiment

$$g(-O_2) \approx 38/100 \text{ eV.}$$

This number is much higher than the corresponding g yield $g(-O_2) = 1.3/100 \text{ eV}$ derived by Gillen et al. [17] at similar dose rates for pure polystyrene. Presumably the shortlived absorption

centers R_2 which react strongly in the presence of oxygen are responsible for the very high value $g(-O_2)$ of BCF-12.

4.3. Absorption spectra for the different absorption centers

One aim of the present chapter is to separate the absorption spectrum $\Sigma_2(\lambda)$ of the shortlived absorption centers R_2 from the contributions $\Sigma_1(\lambda)$, $\Sigma_P(\lambda)$ of the other absorption centers (R_1, P). This can be best done at very low doses ($D \rightarrow 0$) when the decay of the unstable centers R_2 is negligible as can be seen from Eqs. (7a) and (11c). According to Eqs. (10) and (13) $\Sigma_2(\lambda)$ is proportional to the cross section $\sigma_2(\lambda)$ for the absorption of photons by R_2 and can be determined from the slope $d(\Delta\mu_2)/dD$ at $D \approx 0$.

The method of analysis will be explained for an arbitrary example given in Fig. 8. If Eq. (16a) is correct the induced absorption $\Delta\mu$ can be written as a sum of two terms. The stable absorption centers (R_1, P) are responsible for one term ($\Delta\mu_1 + \Delta\mu_P = (\Sigma_1 + \Sigma_P) \cdot D$) which rises linearly with exposure time t and dose $D = \dot{D} \cdot t$, while the contribution $\Delta\mu_2$ of the unstable absorption centers R_2 saturates. For $\lambda_0 = 580 \text{ nm}$ (Fig. 8(b)) we find $\Delta\mu(t) \approx \text{const}$ for $t > 90 \text{ h}$ and consequently $\Sigma_1(\lambda_0) \cong \Sigma_P(\lambda_0) \approx 0$. For $\lambda_1 = 420 \text{ nm}$ (Fig. 8(a)) one can calculate $\Sigma_1(\lambda_1) + \Sigma_P(\lambda_1) = d(\Delta\mu)/dD$ from the linear part of the curve $\Delta\mu(t)$ for $t > 90 \text{ h}$. The difference $\Delta\mu - \Delta\mu_1 - \Delta\mu_P$ in Fig. 8(a) has

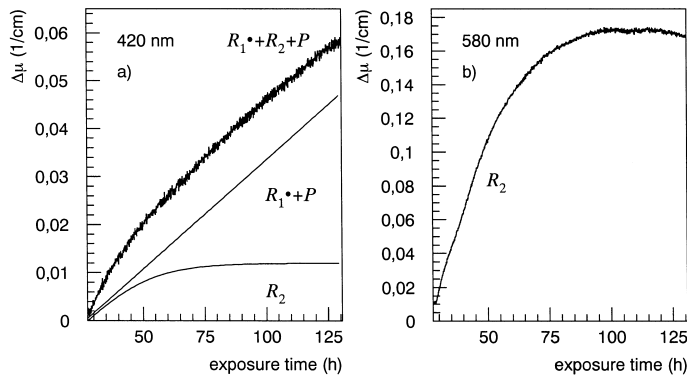


Fig. 8. Separation of the induced absorption $\Delta\mu$ measured during irradiation in argon at $\lambda = 420 \text{ nm}$ into contributions from the stable absorption centers ($P + R_1$) and the unstable ones (R_2). The curves labeled R_2 in (a) and (b) have the same time dependence, only the normalization is different ($D = 1.26 \text{ kGy}$, $\dot{D} = 10.5 \text{ Gy/h}$, argon atmosphere).

the same time dependence as the curve in Fig. 8(b) and can therefore be attributed to R_2 . The analysis for different wavelengths in the range $\lambda = 420\text{--}650$ nm showed that the reaction parameter κ_2 is independent of λ . An important conclusion is that one needs only three classes of absorption centers (P, R_1, R_2) to reproduce the measured absorption curves. In the present work we do not separate the contributions of R_1 and P . In principle this could be done if one introduces oxygen into the vacuum chamber as can be seen from Fig. 3(a).

The results for irradiations in argon atmosphere are presented in Figs. 9(a) and (b). Fig. 9(a) shows the absorption spectra $\Sigma_2(\lambda)$ and $(\Sigma_1(\lambda) + \Sigma_P(\lambda))$ for the case $[O_2] = 0$, i.e., when there was no oxygen dissolved in the fiber, while the corresponding spectra $\Sigma'_2(\lambda)$, $(\Sigma'_1(\lambda) + \Sigma'_P(\lambda))$ for the case $[O_2] \neq 0$ are plotted in Fig. 9(b).

The following two interesting consequences can be derived from Figs. 9(a) and (b).

1. The spectral distributions Σ_2 and Σ'_2 are practically equal: $\Sigma_2(\lambda) \approx \Sigma'_2(\lambda)$. From the definition of Σ_2 (see Eq. (13)) one can conclude that the shortlived absorption centers R'_2 and R_2 formed with and without oxygen must be identical. The cross sections for the absorption of photons must be the same ($\sigma_2(\lambda) = \sigma'_2(\lambda)$), and the same holds for the chemical yield ($g_2 \approx g'_2$). From the latter one can conclude that the shortlived absorption centers are stable at low concentrations $[R_2]$ even in the presence of O_2 . They decay only at higher concentrations via a bimolecular reaction ($R_2 + R_2 \rightarrow X$).

2. We further see that $(\Sigma_1 + \Sigma_P) \gg (\Sigma'_1 + \Sigma'_P)$. This is due to the fact that radicals (R_1) decay rapidly in the presence of oxygen. In the following we will assume $\Sigma'_1(\lambda) \equiv 0$.

This interpretation is confirmed by Fig. 9(c) which summarizes the results from irradiations in air. The permanent damage $\Delta\mu_p$ remaining after the end of annealing in air has been determined for two different irradiations. By comparison of Figs. 9(b) and (c) one obtains: $\Delta\mu_p/D \equiv \Sigma'_P(\lambda) \approx \Sigma'_P(\lambda) + \Sigma'_1(\lambda)$. This relation can only be correct if $\Sigma'_1(\lambda) \approx 0$.

In addition the slope parameter $\Sigma'(\lambda) = d(\Delta\mu)/dD$ at $D \approx 0$ is plotted in Fig. 9(c) for the irradiations in air. It is of similar size as the

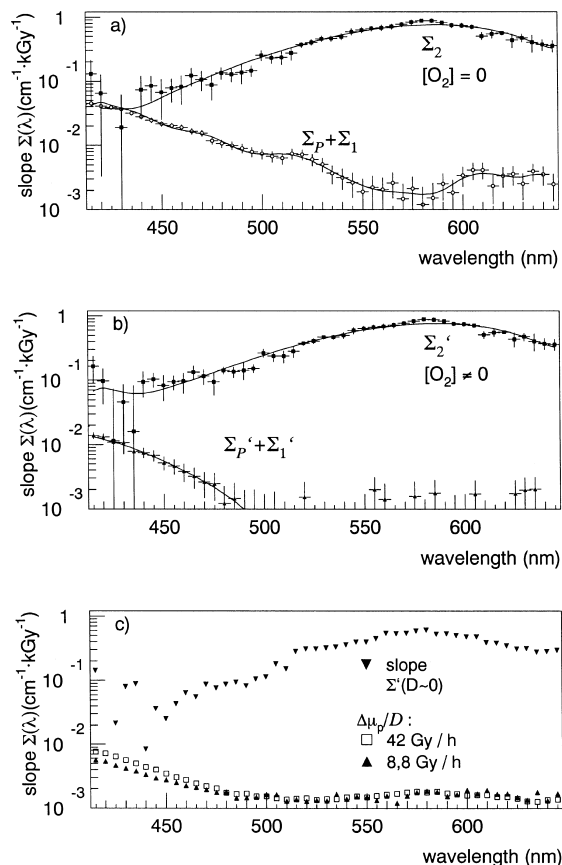


Fig. 9. (a),(b) Absorption spectra $\Sigma_i(\lambda)$ for the different absorption centers of BCF-12 determined from measurements in argon. Σ'_i and Σ_i refer to the two cases with and without dissolved oxygen. (c) The slope parameters $\Delta\mu_p/D$ ($\Delta\mu_p$ = permanent damage) after irradiation and annealing of BCF-12 in air (doses $D = 1.1\text{--}2.5$ kGy) and $\Sigma' = d(\Delta\mu)/dD$ at $D \approx 0$.

corresponding parameters Σ_2 and Σ'_2 in Figs. 9(a) and (b). This shows again that the absolute value of the oxygen concentration has only little influence on the concentration of shortlived absorption centers R_2 .

4.4. Fluorescence light yield of BCF-12

During all irradiations of the present work the fluorescence light produced by the X-rays in the fiber was registered [7]. In addition calculations were performed under the following simplifying assumptions [12] in order to quantify the influence

of radiation induced absorption on the light yield emitted by the fiber.

1. The primary light yield is emitted isotropically with a spectral distribution as given by BICRON [13]. It does not change during irradiation.
2. The fiber is irradiated uniformly along its length with a constant dose rate \dot{D} . The absorption coefficient $\mu_0(\lambda)$ before irradiation and the radiation induced absorption $\Delta\mu(\lambda, t)$ were determined from the data of the present experiment. At each moment before, during and after irradiation the integration was carried out over the whole fluorescence spectrum.
3. The spectral efficiency of the photomultiplier tube (HAMAMATSU R 955) was taken into account.

Tests showed that the calculated results are in good agreement with experimental data [12]. A special example is plotted in Fig. 10. A 30 cm long BCF-12 fiber, which has a mirror at one end, is exposed to a uniform background radiation ($\dot{D} = 42$ Gy/h). The pulse height of particles hit-

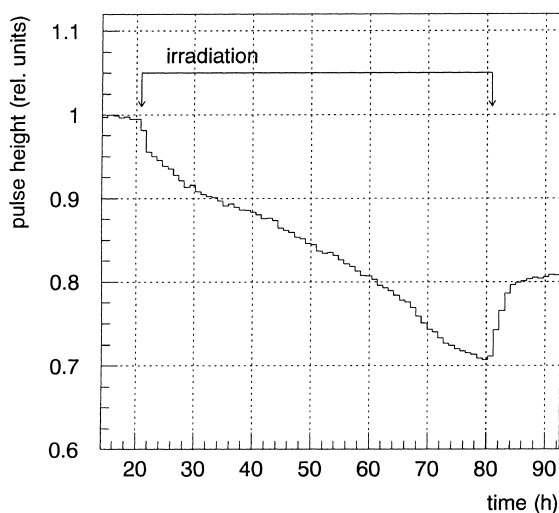


Fig. 10. Influence of damage due to a background radiation on the pulse height produced by particles which deposit a certain amount of energy in the middle of a 30 cm long BCF-12 fiber. The decrease of light yield during and after irradiation is plotted as a function of time. The fiber has a mirror at one end. The influence of uniform irradiation of the whole fiber in air has been calculated using the experimentally determined induced absorption $\Delta\mu(\lambda, t)$ ($D = 2.5$ kGy, $\dot{D} = 42$ Gy/h, exposure time $t = 21$ – 81 h).

ting the middle of the fiber is plotted as a function of time during and after irradiation. The permanent damage remaining after the end of the recovery process ($t \approx 90$ h) dominates, it increases smoothly during irradiation. On the other hand the pulse height decreases rapidly by about 4% during the first hour of irradiation ($t = 21$ – 22 h). This effect can be attributed to the shortlived absorption centers. Their concentration saturates after one hour of irradiation in air. The effect is relatively small (in an oxygen free atmosphere it would be 13 times larger, see Section 4.1), but the change occurs in a very short time.

In the following we consider only the influence of shortlived absorption centers R_2 on the detector calibration. The essential effect will be that the calibration will slightly depend on the dose rate \dot{D} . The maximum relative change of pulseheight $\Delta I/I_0$ due to the shortlived absorption centers R_2 alone can be roughly estimated from Eq. (9) if one assumes that the mean wavelength of the fluorescence spectrum is $\bar{\lambda} \approx 450$ nm. For irradiations in air (with $\dot{D} < \dot{D}_{\text{crit}}$) one obtains approximately

$$\begin{aligned} \left| \frac{\Delta I}{I_0} \right| &\approx \ell \cdot \Delta\mu_{2S}(\bar{\lambda}, \dot{D}) \\ &= 2.6 \cdot 10^{-4} \cdot \ell [\text{cm}] \cdot \sqrt{\dot{D}[\text{Gy/h}]}, \end{aligned} \quad (19)$$

where ℓ is the path length of the light in the irradiated part of the fiber. The results obtained with Eq. (19) agree quite well those of the detailed calculations mentioned above. For a detector using BCF-12 fibers of 30 cm length Eq. (19) yields $\Delta I/I_0 = 1\%$ for $\dot{D} = 1.7$ Gy/h. Under these conditions the calibration of the detector with and without beam background will differ by about 1%. Saturation will be achieved after about 8 h corresponding to an absorbed dose of ~ 14 Gy. Only in relatively long fibers and at high dose rates one will expect effects $|\Delta I/I_0| \gg 1\%$.

5. Discussion

In Section 4 it has been shown that the measured data can be described quantitatively if one assumes that three classes of absorption centers

(P, R_1, R_2) are produced in BCF-12 during irradiation. In Section 5.1 it will be discussed what we presently know about the nature of the absorption centers. BCF-12 has a polystyrene core, hence the results of the present analysis will be first compared with those of pure polystyrene. Section 5.2 summarizes the processes which have been derived from the analysis of the data.

5.1. Nature of absorption centers

γ irradiated polystyrene was investigated by different authors. From ESR studies at least two distinct radical species were identified [14]: The disubstituted benzyl radical (chemical yield $g_1 = 0.09$ per 100 eV) and the cyclohexadienyl radical ($g_2 = 0.009/100$ eV). Optical investigations were performed by Bross and Pla-Dalmau [15] and by Wallace et al. [9] after exposure to γ rays from a ^{60}Co source. In both experiments the transmission of pure polystyrene samples was measured. Bross et al. irradiated the samples in an oxygen free atmosphere (nitrogen) at doses $D = 10\text{--}1000$ kGy (1–100 Mrad) and a high dose rate $\dot{D} = 10$ kGy/h. From their data we have determined the radiation induced absorption, namely the initial damage $\Delta\mu_i$ directly after the end of irradiation and the permanent damage $\Delta\mu_p$ after annealing in air. At not too high doses ($D \lesssim 50$ kGy) $\Delta\mu_i$ and $\Delta\mu_p$ are proportional to the absorbed dose D and the slope parameters $\Delta\mu_i/D$ and $\Delta\mu_p/D$ plotted in Fig. 11 depend only on the wavelength λ .

In the following we try to show that the radicals R_1 identified in BCF-12 are identical with those detected in polystyrene. A first indication is the small peak occurring at $\lambda = 520$ nm in the lower curve of Fig. 9(a). It is more clearly visible in Fig. 3(c). This peak can be attributed to R_1 since it is not found in the permanent damage (see Fig. 3(c)). The same peak was observed in polystyrene by Bross et al. and by Wallace et al. in the annealable part of the induced absorption, which is attributed to the radicals R produced in polystyrene. In the logarithmic representation of Fig. 11 the peak is only weakly visible at $\lambda = 525$ nm. A further confirmation of the hypothesis that R and R_1 are identical can be obtained if one considers the wavelength dependence in BCF-12 and polysty-

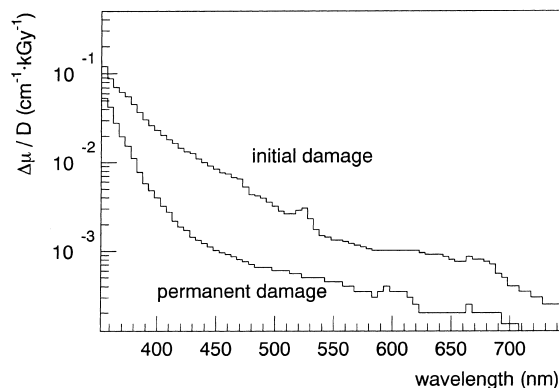


Fig. 11. Wavelength dependence of the initial ($\Delta\mu_i$) and permanent damage ($\Delta\mu_p$) in pure polystyrene. The ratios $\Delta\mu_i/D$ and $\Delta\mu_p/D$ (dose $D = 50$ kGy) were calculated from data of Bross and Pla-Dalmau [14]. The small peak at $\lambda = 525$ nm was also observed in BCF-12 (see Fig. 3(c)).

rene. From a comparison of Figs. 9(a), (b) and 11 in the range 420–540 nm one obtains that the annealable parts of the radiation induced absorption $\Delta\mu$ are proportional to each other and of similar order of magnitude. At the same dose the radical concentration $[R_1]$ in BCF-12 seems to be roughly twice as high as in polystyrene. We now also understand why the radicals R_1 formed in BCF-12 are stable at low doses $D \leq 2.5$ kGy: saturation effects due to bimolecular reactions are expected in polystyrene only at much higher doses $D \geq 100$ kGy [14].

The nature of the shortlived absorption centers R_2 observed in BCF-12 is still not known. Fig. 11 shows no evidence for an absorption band in polystyrene in the range $\lambda = (550\text{--}750)$ nm. In an independent experiment [16] shortlived absorption centers were also observed in the scintillating fiber SCSF81(Y7). However, the peaks of the new absorption bands detected in the two investigated fibers occur at different wavelengths ($\lambda = 580$ nm for BCF-12 and $\lambda = 630$ nm in SCSF81(Y7)). Hence, it seems to be more probable that R_2 has to be attributed to the fluors in the scintillator and not to the polystyrene matrix. Further experiments are necessary. Pure polystyrene fibers should be studied. Presently we try to find out by means of ESR measurements whether R_2 is a radical.

Finally a short remark concerning peroxy radicals ($\text{RO}_2\cdot$) should be made. ESR studies have shown that they are formed when polymers or plastic scintillators are irradiated in the presence of oxygen. They are unstable and at room temperature they usually decay within hours according to reactions (3)–(6). In BCF-12 only one unstable type of absorption center (R_2) was detected. R_2 cannot be the peroxy radical since it was also observed when no oxygen was available. Within the experimental errors there is no evidence that the peroxy radicals produced in BCF-12 absorb visible light ($\lambda = 420\text{--}650\text{ nm}$).

5.2. Summary

The behaviour of the scintillating fiber BCF-12 was systematically studied during and after irradiation with X-rays. The analysis of the data was very successful, since a quantitative understanding of the reaction mechanism was achieved. The radiation induced absorption can be reproduced quantitatively [12] using the formulae described in Section 3. Only two free parameters have to be fitted to describe the kinetics of the shortlived absorption centers. Since the dose rate dependence measured in the range 8–42 Gy/h is reproduced correctly, one can predict the radiation induced absorption in a much wider range than was studied in the present experiment.

The absorption spectrum of the shortlived absorption centers (R_2) and especially its overlap with the fluorescence spectrum of BCF-12 was determined from the data. Due to the different kinetics the contributions of different absorption centers could be separated. This allowed to determine the influence of R_2 on the emitted fluorescence light yield. Visible effects are expected mainly at dose rates $\dot{D} \geq 1\text{ Gy/h}$.

The method to investigate radiation damage not only after, but also during irradiation revealed surprising effects. Saturation of absorption was observed and sharp kinks occurred in the transmission curves when the oxygen dissolved in the fiber was consumed due to reactions with radicals. It is interesting to compare radicals and shortlived absorption centers R_2 . Radicals decay at once ($\text{R}\cdot + \text{O}_2 \rightarrow \text{RO}_2\cdot$) when oxygen is dissolved in the

scintillator matrix, while R_2 is stable even in the presence of oxygen at least at low concentrations $[\text{R}_2]$. This can be learned from the behaviour of R_2 at very low doses when the decay of R_2 is negligible. The absorption spectra of R_2 for the two cases $[\text{O}_2] = 0$ and $[\text{O}_2] \neq 0$ are identical ($\Sigma_2(\lambda) \approx \Sigma'_2(\lambda)$). With and without oxygen R_2 decays only at higher concentrations $[\text{R}_2]$ via a bimolecular reaction:



The radiation oxidation scheme of R_2 seems to be much simpler than that of radicals (see Eqs. (3)–(6)). The surprise was that the reaction parameter κ_2 changes suddenly by a factor 200, when the limit $[\text{O}_2] \rightarrow 0$ is reached ($\kappa'_2/\kappa_2 = 204 \pm 50$). The absolute concentration $[\text{O}_2]$ has only little influence on κ'_2 , the reaction parameter depends practically alone on the fact whether oxygen is available or not. This must be due to the high mobility of O_2 molecules in the polystyrene matrix.

The saturation values of the induced absorption $\Delta\mu_{2S}$ and $\Delta\mu'_{2S}$ for the two cases $[\text{O}_2] = 0$ and $[\text{O}_2] \neq 0$, respectively, are strongly different. For equal dose rates and equal wavelengths one obtains from Fig. 6, $\Delta\mu_{2S}/\Delta\mu'_{2S} \approx 13$. This is in quite a good agreement with Eq. (11b) which predicts (for $\Sigma_2 = \Sigma'_2$)

$$\Delta\mu_{2S}/\Delta\mu'_{2S} = \sqrt{\kappa'_2/\kappa_2} \approx 14.$$

The distinct properties of radicals and shortlived absorption centers have direct consequences for the use of the BCF-12 fiber in a detector. The creation of the strongly absorbing radicals during irradiation can be avoided if one guarantees that $[\text{O}_2] \neq 0$ in the whole fiber. The formation of shortlived absorption centers R_2 cannot be avoided in the same manner but nevertheless the saturation concentration can be reduced by a factor 13 if $[\text{O}_2] \neq 0$. The availability of oxygen is important to reduce the radiation sensitivity, hence glueing of the fibers which inhibits the oxygen diffusion should be avoided.

Acknowledgements

This work has been supported by the German Federal Ministry for Education, Science, Research and Technology (BMBF) under the contract 05 7HH 19P.

References

- [1] J.L. Bolland, *Quart. Rev. Chem. Soc.* 3 (1949) 1.
- [2] R.L. Clough, K.T. Gillen, M. Dole, Radiation resistance of polymers and composites, in: D.W. Clegg, A.A. Collyer (Eds.), *Radiation effects on Polymers*, Elsevier, Amsterdam, 1991.
- [3] R.L. Clough, J.S. Wallace, Radiation effects on organic scintillators: Studies of color center annealing, in: T. Dombek, V. Kelly, G. Yost (Eds.), *Symposium on Detector Research and Development for the Superconducting Super Collider*, World Scientific, New York, 1990, p. 661.
- [4] B. Wulkop, K. Wick, W. Busjan, A. Dannemann, U. Holm, *Polymer Preprints* 35 (1994) 924.
- [5] B. Wulkop, K. Wick, W. Busjan, A. Dannemann, U. Holm, *Nucl. Instr. and Meth. B* 95 (1995) 141.
- [6] B. Wulkop, K. Wick, W. Busjan, A. Dannemann, U. Holm, *Nucl. Phys. B (Proc. Suppl.)* 44 (1995) 542.
- [7] W. Busjan, K. Wick, T. Zoufal, *Nucl. Phys. B (Proc. Suppl.)* 61B (1998) 504.
- [8] AIC Software, Grafton, Mass. 01519, USA.
- [9] J.S. Wallace, M.B. Sinclair, K.T. Gillen, R.L. Clough, *Rad. Phys. Chem.* 41 (1993) 85.
- [10] B. Biçken, U. Holm, T. Marckmann, K. Wick, M. Rohde, *IEEE Trans. Nucl. Sci.* 38 (1991) 188.
- [11] K. Wick, D. Paul, P. Schröder, V. Stieber, B. Biçken, *Nucl. Instr. and Meth. B* 61 (1991) 472.
- [12] W. Busjan, Thesis, University of Hamburg, 1997; Internal report DESY F35D-97-09 (1997).
- [13] BICRON Corporation, Newbury, Ohio, catalogue, 1990.
- [14] L.A. Harrah, in: G. Alder (Ed.), *Organic Solid State Chemistry*, Gordon and Breach Science, New York, 1969, p. 197.
- [15] A. Bross, A. Pla-Dalmau, *ACS-Symposium Series: Radiation Effects on Polymers*, 1991, p. 475.
- [16] W. Busjan, K. Wick, T. Zoufal, *Proc. IRaP'98*, *Nucl. Instr. and Meth. B*, to be published.
- [17] K.T. Gillen, J.S. Wallace, R.L. Clough, *Rad. Phys. Chem.* 41 (1993) 101.